

Non-locality in the nucleon-nucleon interaction and nuclear matter saturation

M. Baldo and C. Maieron

INFN, Sezione di Catania, Via Santa Sofia 64, 95123 Catania, Italy

(Dated: November 5, 2018)

We study the possible relationship between the saturation properties of nuclear matter and the inclusion of non-locality in the nucleon-nucleon interaction. To this purpose we compute the saturation curve of nuclear matter within the Bethe-Brueckner-Goldstone theory using a recently proposed realistic non-local potential, and compare it with the corresponding curves obtained with a purely local realistic interaction (Argonne v_{18}) and the most recent version of the one-boson exchange potential (CD Bonn). We find that the inclusion of non-locality in the two-nucleon bare interaction strongly affects saturation, but it is unable to provide a consistent description of few-body nuclear systems and nuclear matter.

PACS numbers: 21.65.+f, 24.10.Cn, 21.30.-x

I. INTRODUCTION

The effective nucleon-nucleon (NN) interaction is expected, on physical grounds, to be intrinsically non-local. The quark structure of nucleons implies that the potential between two interacting nucleons cannot be expressed only in terms of the center of mass degree of freedom, at least for distances smaller than twice the nucleon radius. Even a description of the NN interaction in terms of one-boson exchange processes introduces some degree of non-locality [1]. For practical purposes, however, it is convenient to have a local (energy independent) NN interaction, to be used in numerical applications. The modeling of the NN interaction by a local potential, with possible guidance from meson exchange processes, has been extremely successful in reproducing the NN experimental phase shifts and deuteron properties [2, 3]. This approach has developed for many years and has reached a high degree of sophistication.

It has been established by now that these local NN potentials, which are essentially phase equivalent, give slightly different results for the three- and four-nucleon systems. Furthermore, in general they underestimate the binding energy and do not give the correct values for some polarization observables. This drawback has been usually overcome by introducing three-body forces, which can be again justified by the non-elementary nature of the nucleon. Actually three-body forces can be generated also by meson-exchange processes of higher order, where the nucleon is excited in the intermediate states of the interaction processes or meson-meson couplings are introduced [4]. Both non-locality and three-body forces can be considered to have a common origin, the inner structure of the nucleon. However, one cannot fully reduce one to another, since non-locality has definite effects already at the two-body level, e.g. a non-local potential cannot be equivalent, in general, to an energy independent local potential. Furthermore, it is not clear to what extent the off-shell behavior of a non-local potential, i.e. the off shell T -matrix, can be simulated by the presence of three-body forces.

Another question where non-locality could play a role

is the mechanism of saturation in nuclear matter. In fact, it turns out that in order to get saturation with a local (energy independent) interaction, it is essential to include a strong repulsive core, as also suggested by the behavior of the NN phase shifts. Again, three-body forces are necessary to tune the saturation point close to the empirical one. It is surely conceivable that a certain degree of non-locality could simulate the strong repulsion at short distance, which is one of the main features of the NN interaction, and maybe reduce the need of three-body forces.

It appears, therefore, of great interest to investigate to what extent non-locality alone could enable to get saturation, possibly close to the empirical one, and at the same time to describe three- and four-body systems correctly.

Recently, in a series of papers by Doleschall and collaborators [5, 6, 7], a new realistic non-local NN potential was proposed, which is able to describe accurately both the NN phase shifts and the properties of three-nucleon systems (${}^3\text{He}$ and ${}^3\text{H}$), i.e. their binding energies and radii. Also the alpha particle appears to be reasonably well described [8]. The need of three-body forces in this case seems to be absent, or completely simulated by the non-locality.

This NN interaction introduces non-locality at short distance ($r \leq 3 \text{ fm}^{-1}$) for the s-wave channels, and possibly also for the p-waves ones [7]. The rest of the potential is taken as the Argonne v_{18} [2], while the non-local part is purely phenomenological.

In this paper we address the issue of the saturation properties of non-local potentials. To this purpose we present nuclear matter calculations within the Bethe-Brueckner-Goldstone method extended up to three hole-line contributions, which is known to converge well and to give an accurate nuclear matter saturation curve.

As the main representative of non-local NN interaction we take the potential of ref. [6]. We compare the corresponding nuclear matter Equation of state (EOS) with those obtained starting from the charge-dependent (CD) Bonn [9] and the v_{18} potentials. The former can be considered the most recent and accurate interaction based on the one-boson exchange model and, therefore,

it contains some degree of non-locality. The latter is a convenient reference local potential for the comparison with Doleschall's, which, as we stated above, coincides with the v_{18} in the $L \geq 1$ channels. Additionally, other modern local potentials, like Argonne v_{14} [3] or Paris potential [10], give similar results, close enough to v_{18} to be considered equivalent for the present purpose [11].

The study of phase-shift equivalent NN interactions and their predictions of nuclear matter saturation properties has a long history. For example in refs. [12, 13] unitarily equivalent interactions which differ in the short range part of the 1S_0 channel were shown to provide rather different values of the saturation energy and density. More recently, the predictions of modern NN potentials were studied in refs. [14, 15, 16]. Here the role of non-locality in the binding energy of nuclear matter was also partially discussed, using the CD Bonn and the Nijmegen-I [17] potentials, which were shown to provide a stronger binding than local potentials such as the v_{18} . However, both these potentials underestimate the binding energy of three- and four-body systems [19], at variance with Doleschall's interaction [6]. Therefore when using the latter we can, in principle, expect different results also for nuclear matter calculations.

It is well known that the saturation points obtained within the Brueckner approximation for the gap choice and different NN interactions tend to lie along a band [11], the celebrated "Coester band", in the energy-density plane. The position inside the band for a given NN interaction turns out to be correlated with the d-state probability in the deuteron. The high-energy, high-density part of the band is usually associated with low values of this probability. However, as shown in ref. [18], this trend does not hold any more if three hole-line contributions are included, as we do in the present paper. In this case the results are quite insensitive to the d-wave probability value and actually close to each other, at least for local potentials or quasi-local potentials like the Paris one. The same conclusion holds true if the continuous choice for the single particle potential is used in the Brueckner approximation [11].

The paper is organized in the following way. In Section II we shortly study the free space properties of the Doleschall, CD Bonn and v_{18} potentials. In Section III, after introducing the BBG formalism, we study the EOS of nuclear matter obtained with Doleschall's potential, addressing, in particular, the issue of the convergence of the hole-line expansion in this case. We then compare this EOS with those obtained starting from the two other potentials. Finally in Section IV we draw our conclusions.

II. LOCAL VS. NON-LOCAL NN POTENTIALS.

Before studying infinite nuclear matter and in order to better understand the role played by the different NN interactions in the nuclear matter calculations of next

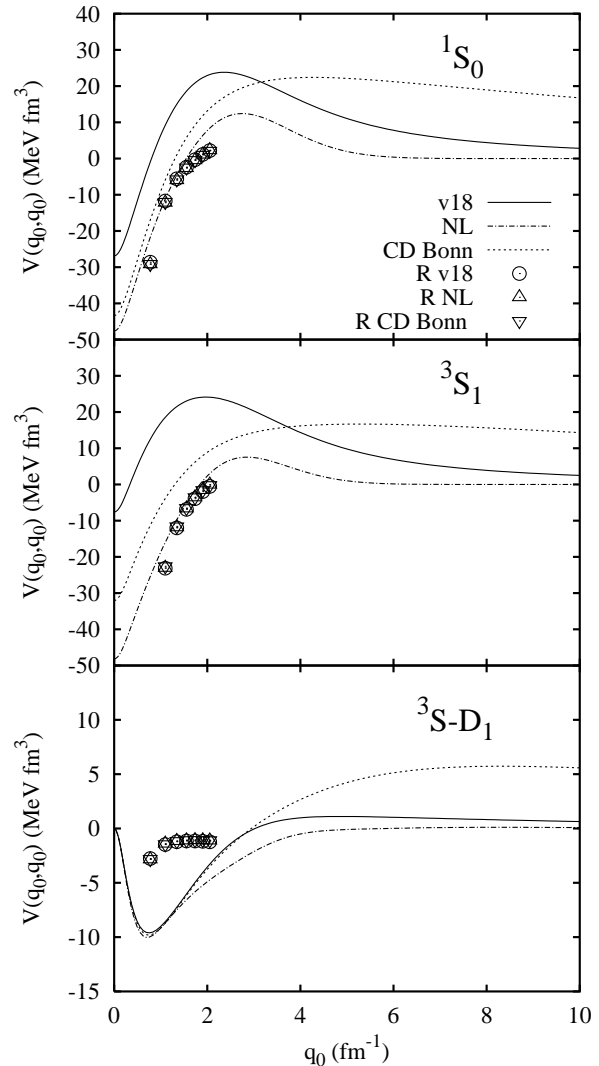


FIG. 1: Diagonal matrix elements of the v_{18} (solid line), CD Bonn (dotted) potentials and of Doleschall's IS potential of ref. [6] (dot-dashed, labeled as NL), for the np interaction in the 1S_0 (upper panel), 3S_1 (middle) and in the coupling 3S_1 - 3D_1 (lower panel) channels. The on-shell $R(q_0, q_0; E)$ R -matrix elements are also shown (symbols), for laboratory energies ranging from 50 to 350 MeV, in steps of 50 MeV.

section, it is useful to briefly compare the properties and characteristics of the potentials we are going to employ, on the basis also of some established results obtained in the literature [2, 9, 14]

The general matrix elements in the momentum representation of a NN interaction $V^c(r, r')$ in a given two-body channel c can be written

$$V_{ll'}^c(k, k') = \frac{2}{\pi} \int r^2 dr r'^2 dr' j_l(kr) V_{ll'}^c(r, r') j_{l'}(k'r') \quad (1)$$

where l, l' are the initial and final orbital angular momenta in the channel, and $j_l, j_{l'}$ the corresponding spher-

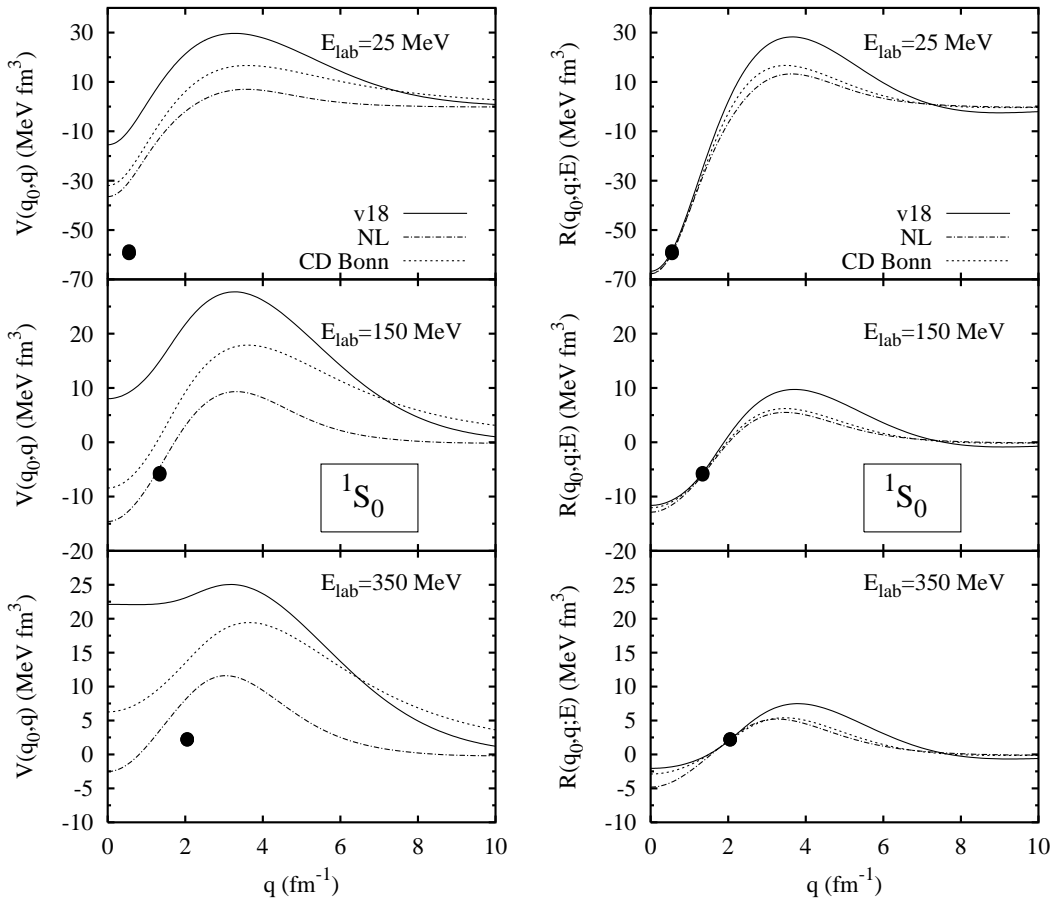


FIG. 2: Left panels: off-diagonal 1S_0 np matrix elements of the v_{18} , CD Bonn and NL potentials, for three fixed momenta q_0 corresponding to laboratory energies $E_{\text{lab}} = 2E = 25$ (upper panel), 150 (middle) and 350 (lower) MeV. Right panels: corresponding half off-shell R -matrix elements. The solid dot marks the on-shell values of the R -matrix.

ical Bessel functions. For a local potential $V^c(r, r') = v^c \delta(r - r')/rr'$. In the momentum representation the matrix elements $V_{ll'}^c(k, k')$ of eq. (1) are in any case a function of two variables, the initial and final relative momenta k and k' . The non-locality is incorporated in a non trivial way in the analytical properties of the matrix elements of the potentials, as well as of the corresponding T -Matrix, or of the real R -Matrix, which is used here for later convenience. The latter describes the free space NN scattering and is obtained by solving the Lippmann-Schwinger equation, which for two nucleons interacting with energy E in the center of mass frame can be written as:

$$R_{ll'}^c(k, k'; E) = V_{ll'}^c(k, k') + \sum_{l''} \mathcal{P} \int_0^\infty q^2 dq V_{ll''}^c(k, q) \frac{M}{ME - q^2} R_{l''l'}^c(q, k'; E), \quad (2)$$

where the symbol \mathcal{P} denotes the principal value integral and M is the free nucleon mass.

For realistic potentials the on-shell R -matrix,

$R(q_0, q_0; E)$ with $q_0 = \sqrt{ME}$, is fixed, to a large extent, by the fitting of the experimental NN phase shifts.

The potentials we consider in the present paper were fit to reproduce the Nijmegen phase shifts [20] for energies up to 350 MeV in the laboratory frame, and therefore give rise to practically identical on-shell values of the R -matrix in this energy range. However, due to their totally different analytical structure, a quite different behavior of the bare NN matrix elements of eq. (1) can be expected, especially when non-local potentials are compared with local ones.

This is illustrated in fig. 1, where the bare NN diagonal matrix elements and the corresponding on-shell R -matrix for the local v_{18} and the non-local CD Bonn are compared with those obtained from the non-local potential indicated as IS in ref. [6] and hereafter referred to as NL. Here the dominant S-wave channels are considered, for which the main non-locality has been introduced in ref. [6]. One can see that, despite the expected agreement of the various interactions on the R -matrix, the behavior of

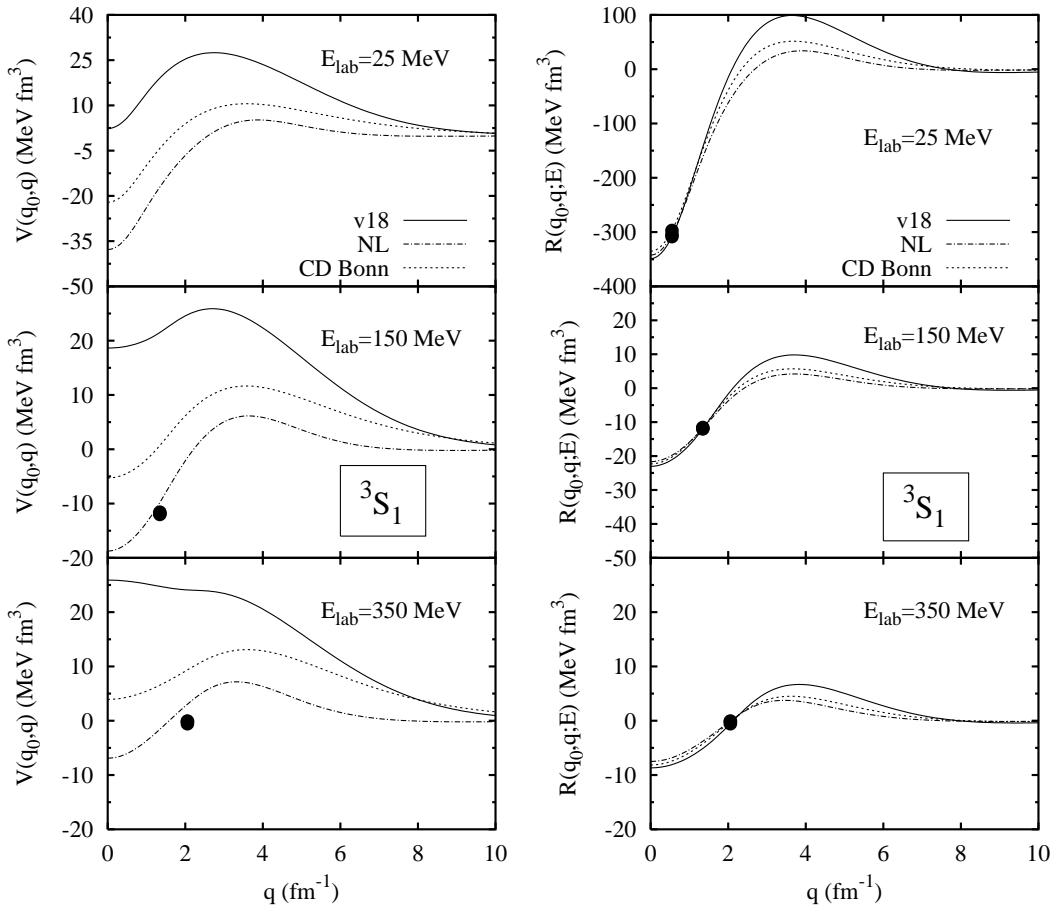


FIG. 3: As fig. 2 but for the 3S_1 matrix elements.

the bare NN matrix elements is quite different. At small momenta we see that in the 1S_0 channel the two non-local potentials are rather close to each other, while they differ significantly from the v_{18} . This is still true in the 3S_1 channel, where, however, the difference between NL and CD Bonn is increased. It can be also seen that at increasing non-locality, i.e. going from the CD Bonn to the NL potential, the deviation from the local potential v_{18} is increasing. This is in agreement with refs. [14, 15], where it was shown that including non-locality makes the attraction provided by the integral term of eq. (2) weaker, thus requiring a less repulsive diagonal matrix element of V , in order to obtain the same on-shell R -matrix. In particular it is interesting to note that the diagonal NL potential is always rather close to the corresponding on-shell R -matrix elements, especially for the 3S_1 channel. In the coupling channel 3S_1 - 3D_1 we see that the three potentials are very close to each other at small momenta, with NL deviating from the others at intermediate q .

Considering the large momentum behavior, we observe that in all cases the CD Bonn potentials exhibits a much larger tail.

Since the diagonal matrix elements of the bare potentials are already so different from each other, it is not surprising then that the off-shell behavior of both the bare V and the R -matrix is also different, as illustrated in figs. 2 and 3, where the half off-shell matrix elements of the bare potentials and of the R -matrix are shown for three choices of the incident energy. The behavior of the bare potentials (left panels in the figures) shows essentially the same features we have already observed for the diagonal matrix elements. The curves representing the R -matrix (right panels) are closer to each other, but still sensible differences are observed, especially when the results corresponding to the v_{18} are compared with the two other non-local potentials.

Finally in fig. 4 we also show the half off-shell V and R 3S - 3D_1 matrix elements. Here only the tensor part of the NN interaction can contribute, which was shown in previous works to be strongly affected by the inclusion of non-locality [14, 15, 16], and which is known to play an important role in nuclear structure calculations. We see that indeed, the inclusion of non-locality reduces the strength of the interaction and, for the NL case, also the

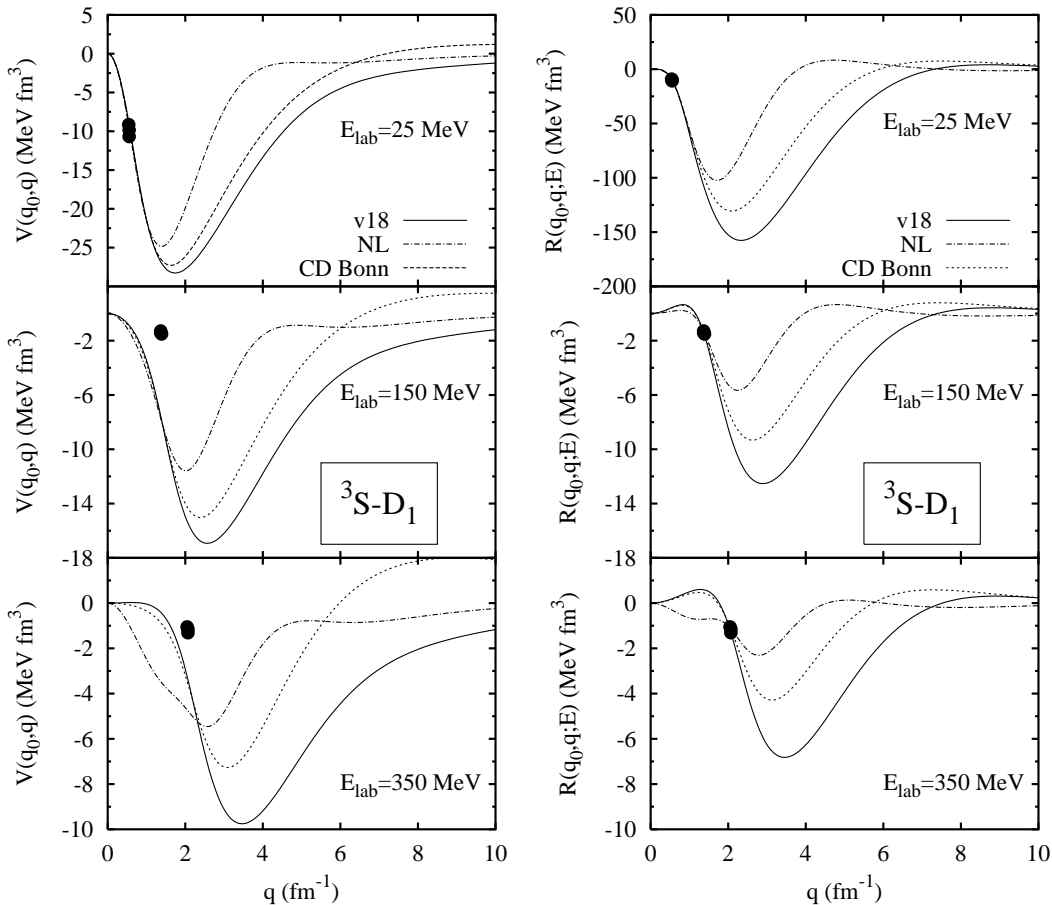


FIG. 4: As fig. 2 but for the ${}^3S_1 - {}^3D_1$ matrix elements.

range of momentum values where the matrix elements are significantly different from zero.

III. EOS OF NUCLEAR MATTER

A. The BBG expansion

The microscopic calculations of nuclear matter Equation of State, i.e. the energy per particle as a function of density, on the basis of realistic interactions has a long history. Theoretical and numerical methods, accurate enough for our considerations, are nowadays available. We will follow the Bethe-Brueckner-Goldstone scheme, which has been proved [11] to be reliable in a wide range of density. In this expansion the original bare NN interaction v is systematically replaced by the G -matrix, which satisfies the integral equation

$$G[\rho; \omega] = v + \sum_{k_a, k_b} v \frac{|k_a k_b\rangle Q \langle k_a k_b|}{\omega - e(k_a) - e(k_b)} G[\rho; \omega], \quad (3)$$

where $e(k)$ is the single particle energy and Q the so-called Pauli operator which projects both intermediate single particle states above the Fermi surface. The diagrams in terms of the G -matrix are then ordered according to the numbers of hole-lines they contain. The introduction of the self-consistent single particle potential $U(k)$ is an essential ingredient of the method

$$U(k) = \sum_{k' < k_F} \langle k k' | G(e(k) + e(k')) | k k' \rangle_A \quad (4)$$

Since $e(k) = \hbar^2 k^2 / 2M + U(k)$, eqs. (3,4) include a self-consistent procedure which determines $U(k)$. In particular we use the continuous choice for the potential $U(k)$, i.e. the definition of eq. (4) is extended to all momenta k , below and above the Fermi momentum k_F . More details can be found in review papers or in textbooks [11]. We extend our calculations up to the three-hole line level of approximation, which has been shown to be accurate in refs. [21, 22, 23] for a variety of NN potentials, including the Argonne v_{14} and v_{18} and the Paris interactions.

However, since Doleschall's NL potential is used here for the first time in BBG calculations of nuclear matter,

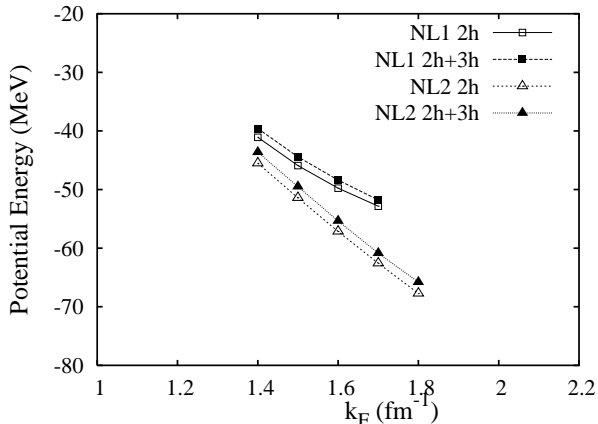


FIG. 5: Potential energy per particle for symmetric nuclear matter calculated with the non-local potentials NL1 (squares), which includes the non-locality in the 1S_0 channel only, and NL2 (triangles), which has the non-locality both in the 1S_0 and in the $^3S_1 - D_1$ channels. Empty symbols correspond to the two hole-line calculations, while full symbols represent the full two + three hole-line results.

before making comparisons of different EOS, we briefly study the accuracy of the BBG expansion in this case. This is done in fig. 5, where the contributions to the binding potential energy of the two hole-line (Brueckner) and three hole-line diagrams are reported. To keep the calculations reliable, the latter has to be substantially smaller than the former.

Two different choices for the NL potential are considered: the curves labeled as NL1 have been obtained using Doleschall's IS potential of ref. [6] only in the 1S_0 channel, while for the curves labeled as NL2 the non-local potential has been included also in the $^3S_1 - ^3D_1$ channel. In the remaining channels the v_{18} interaction has been used.

The three hole-line contributions turn out to be slightly larger than in the case of local potentials (see [21, 22, 23]). However these corrections always remain within 2-3.5% for the NL1 case and within 2.5-4% for NL2, thus indicating that our calculations up to three hole-lines can be considered accurate. It is interesting to note that with the non-local potentials the corrections to the BHF curves are positive, contrary to the case of the v_{18} , where, in the region $1.4 < k_F < 2 \text{ fm}^{-1}$ the three hole-line contributions tend to make the EOS more attractive.

B. Nuclear matter saturation properties

Having established the validity of our calculations, we can now turn our attention to the study of the saturation properties of nuclear matter. To better understand the role that the different potentials we studied in section II play in the nuclear matter EOS it is useful to rewrite the

Bethe-Goldstone equation (3) in the channel c ,

$$\langle kl | G^c(\rho, \omega) | k'l' \rangle = V_{ll'}^c(k, k') + \sum_{l''} \int_0^\infty q^2 dq V_{ll''}^c(k, q) \frac{\overline{Q}(q)}{\omega - \overline{E}(q)} \langle ql'' | G^c(\rho, \omega) | k'l' \rangle, \quad (5)$$

where, following standard procedures [11], we have introduced the angle averaged expressions of the Pauli operator, \overline{Q} , and of the energy, \overline{E} , in the denominator of the integral term. Eq. (5) closely resembles the Lippmann-Schwinger equation (2), the difference being due to the presence, in the former, of the Pauli blocking operator and of a different energy denominator. Both these terms produce a quenching of the integral term contribution in the Bethe-Goldstone equation with respect to the Lippmann-Schwinger case. Therefore the behavior of the G-matrix is expected to be rather similar to that of the R-matrix, with this quenching effect being weaker for the non-local potentials, for which the integral term is already small.

Since the non-locality in the NL potential is introduced in the 1S_0 and in the coupled $^3S_1 - ^3D_1$ channels, we begin by studying the contributions of these channels to the potential binding energy per particle. This is done, at the Brueckner level, in fig. 6, where the results corresponding to the non-local CD Bonn (empty dots/dashed line) and NL potentials (triangles/dot-dashed) are compared with the v_{18} (crosses/solid). In agreement with the discussion in section II, where we compared bare potentials and R-matrix elements, we observe that in the 1S_0 channel the CD Bonn and NL potential contributions are very close to each other and that they provide additional binding, with respect to the v_{18} case. When we consider the 3S_1 and 3D_1 channels, again we see that the non-local potentials provide more binding, but in this case the NL curve is significantly lower than the CD Bonn one. Since the contributions from all other channels are very similar for the three potentials (with differences of the order of 1 MeV at the largest densities considered here), the differences observed in the 1S_0 and 3S_1 and 3D_1 channels determine the behavior of the total binding potential energy, shown in the bottom panel of fig. 6.

In order to get further insight on the origin of the differences in the potential binding energy, in fig. 7 we also show the potential $U(k)$ for three different choices of the density, namely $k_F = 1.4, 1.6$ and 1.8 fm^{-1} . The most important contribution to the total binding energy comes from the low k region, where the NL potential is, indeed, lower than the others. At large k the behavior of the CD Bonn curve differs from the others, which is not surprising considering the different high momentum tail of the potential V shown, for example, in fig. 1. However this behavior does not seem to affect the final result for the binding energy.

Finally, the saturation curve of nuclear matter is shown in figure 8, where, in order also to make contact with the existing literature, *e.g.* [14, 15, 16], in the upper panel we show results at the Brueckner level, while in the lower

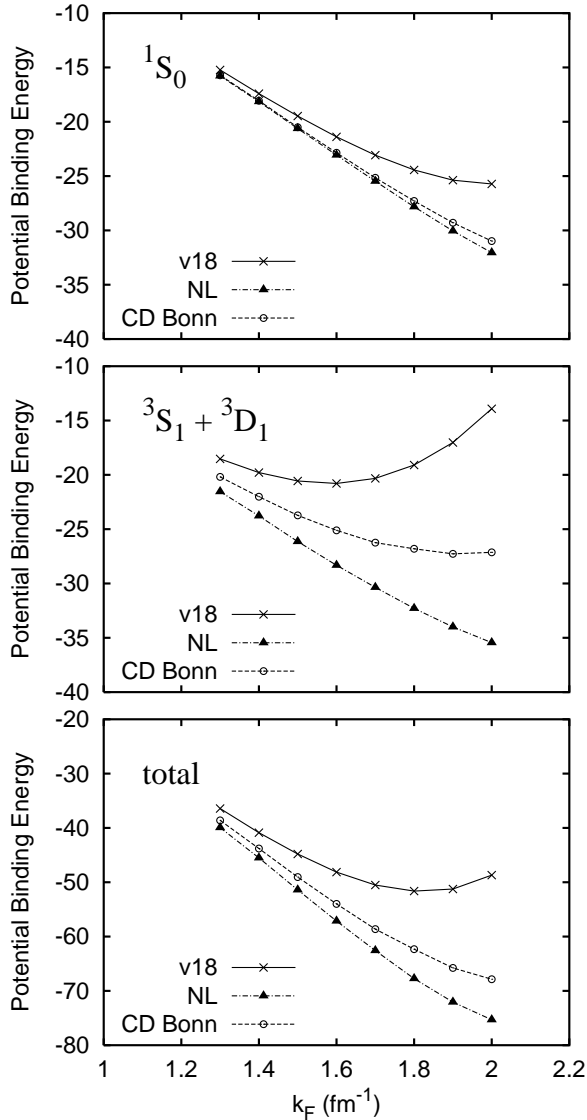


FIG. 6: Contributions of the different channels to the potential binding energy per particle (in MeV) vs. the Fermi momentum k_F . The upper panel corresponds to the 1S_0 channel, the middle panel to the $^3S_1 + ^3D_1$ channels, while the lower panel shows the total potential binding energy. All curves are calculated at the 2 hole-line level.

panel we include contributions at the three-hole line level.

Again, as a reference curve we take the one obtained using the Argonne v_{18} interaction (solid line): as it is well established, the saturation density it gives is slightly larger than the empirical one, and three-body forces can be introduced to correct for this drawback [11, 24]. This is just the issue we want to address, and therefore all the calculations will be presented without the introduction of three-body forces, in order to see to what extent the non-locality can affect this result and in which direction. The discrepancy of the calculated saturation point from the

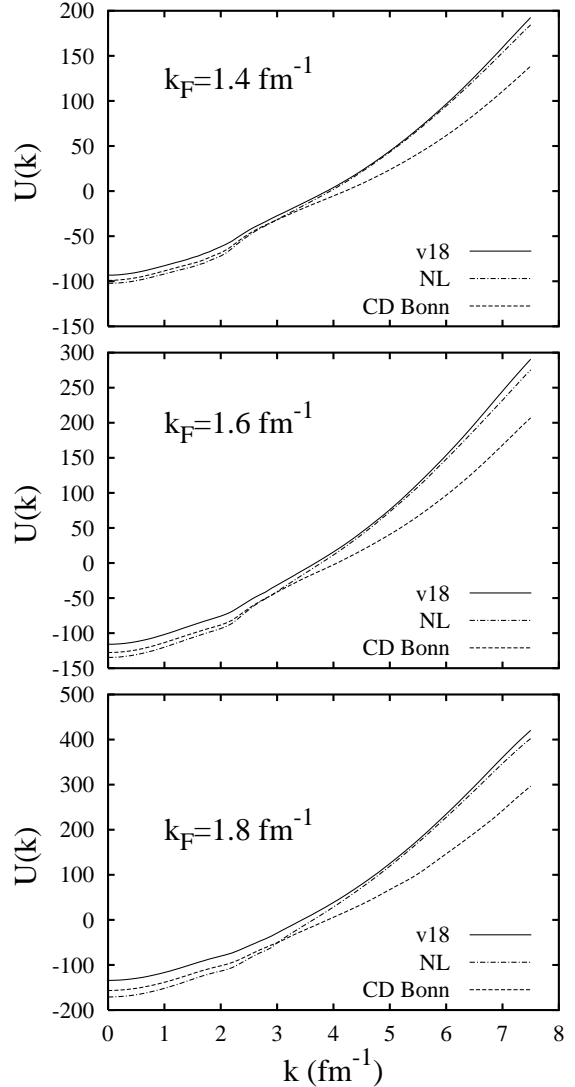


FIG. 7: Potential $U(k)$ (MeV) of eq. (4) for $k_F = 1.4$ (upper panel), 1.6 (middle) and 1.8 fm^{-1} (lower) and for the v_{18} (solid line), non-local (dot-dashed) and CD Bonn (dashed) potentials.

empirical one can be taken as a measure of the amount of three-body forces which is needed. Also relativistic effects can shift the saturation point, as described within the Dirac-Brueckner (DB) approach [1]. However, it has been shown in ref. [25] that the relativistic effects introduced in DB calculations can be described in terms of non-relativistic three-body forces due to virtual creation of nucleon-antinucleon pairs.

Let us now consider the other two interactions, which display different degrees of non-locality. The CD Bonn at the Brueckner level has been already studied in ref. [26] and more recently in ref. [27]. The corresponding saturation curve reported in fig. 8 is in agreement with previous studies. The saturation density and energy are

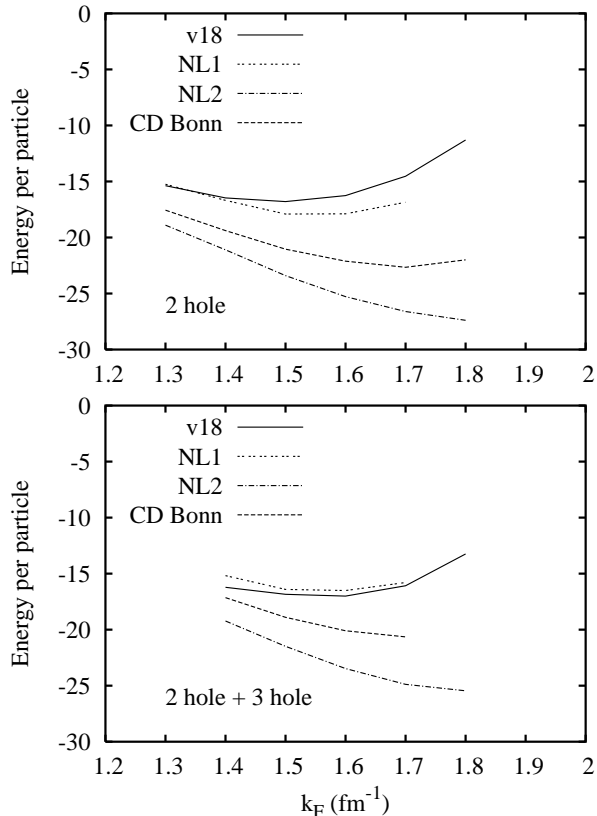


FIG. 8: Energy per particle (in MeV) for symmetric nuclear matter calculated for the v_{18} and CD Bonn potentials and for the non-local interactions NL1, which includes the non-locality in the 1S_0 channel only, and NL2, where the non-locality is included both in the 1S_0 and in the $^3S-D_1$ channels. The upper panel shows results at the two hole line level, while in the lower panel three hole-line contributions are included.

substantially larger than for v_{18} .

The introduction of three hole-line contributions slightly improves the situation, since the three hole-line diagrams give an overall additional repulsion, which however is much smaller than the two hole-line contribution. As shown in the bottom panel of fig. 8, the binding energy decreases, but still remaining too large with respect to the empirical value, while the saturation density is essentially unchanged. All that indicates that, in order to

get the correct saturation point, one needs an amount of three-body force larger than in the v_{18} case. This is somehow at variance with the results for few nucleon systems, where the CD Bonn seems to produce binding energies closer to the experimental ones [19].

The Doleschall' s potential moves further in this direction. As in fig.5 we consider again the NL1 and NL2 cases. The saturation density, as one can see in fig. 8, is larger than in the v_{18} case already for the NL1 curve and it becomes abnormally large when both 1S_0 and $^3S-D_1$ channels include non-locality (NL2), with the energy per particle going down to about -26 MeV. The very large strength for the three-body forces needed in this case, for shifting the saturation curve close to the phenomenological one, is in sharp contrast with the excellent results obtained [5, 6, 7, 8] for few body systems, where virtually no three-body forces are needed.

It looks that any increase of the non-locality would improve the fitting of the binding for the few body, but would shift the saturation point to higher density and binding energy.

IV. CONCLUSION

We have analyzed the effects of the non-locality of the NN interaction on the saturation curve of nuclear matter by considering a set of interactions with different degree of non-locality. While the introduction of non-locality is able to improve the agreement with phenomenology in few-body systems, where it can reduce or even eliminate the need of three-body forces, in nuclear matter we observe a parallel shift of the saturation point in the wrong direction, away from the empirical saturation point. The presence of non-locality seems to be unable to solve one of the fundamental problem in the many-body description of nuclear systems, i.e. the (in)consistency of the three-body forces needed in few-body nuclear systems and in nuclear matter.

Acknowledgments

We thank P. Doleschall and R. Machleidt for providing the subroutines for the non-local and, respectively, the CD Bonn potentials. We would also like to thank P. Schuck for illuminating discussions on the problem of non-locality, which stimulated the present work.

-
- [1] R. Machleidt, *Advances in Nuclear Physics*, Vol. 19, 189 (1989), J.W. Negele and E. Vogt Eds., Plenum NY.
 [2] R. B. Wiringa, V. G. J. Stoks and R. Schiavilla, *Phys. Rev. C* **51**, 38 (1995).
 [3] R. B. Wiringa, R. A. Smith and T. L. Ainsworth, *Phys. Rev. C* **29**, 1207 (1984).

- [4] A. Lejeune, P. Grangé, M. Martzoff, and J. Cugnon, *Nucl. Phys.* **A453**, 189 (1986).
 [5] P. Doleschall and I. Borbely, *Phys. Rev. C* **62**, 054004 (2000).
 [6] P. Doleschall, I. Borbely, Z. Papp and W. Plessas, *Phys. Rev. C* **67**, 064005 (2003).

- [7] P. Doleschall, Phys. Rev. C **69**, 054001 (2004).
- [8] R. Lazauskas and J. Carbonell, Phys. Rev. C **70**, 044002 (2004).
- [9] R. Machleidt, Phys. Rev. C **63**, 024001 (2001).
- [10] M. Lacombe, B. Loiseau, J. M. Richard, R. Vinh Mau, J. Cote, P. Pires and R. de Tourreil, Phys. Rev. C **21**, 861 (1980).
- [11] see for example *Nuclear Methods and the Nuclear Equation of State*, edited by M. Baldo, World Scientific, Singapore, 1999.
- [12] F. Coester, S. Cohen, B. Day and C.M. Vincent, Phys. Rev. C **1**, 769 (1970).
- [13] P. U. Sauer, Ann. Phys **80**, 242 (1973).
- [14] L. Engvik, M. Hjorth-Jensen, R. Machleidt, H. Muther and A. Polls, Nucl. Phys. A **627**, 85 (1997).
- [15] R. Machleidt, "Nuclear forces and nuclear structure," arXiv:nucl-th/9809069.
- [16] R. Machleidt, F. Sammarruca and Y. Song, Phys. Rev. C **53**, 1483 (1996).
- [17] V. G. J. Stoks, R. A. M. Klomp, C. P. F. Terheggen and J. J. de Swart, Phys. Rev. C **49**, 2950 (1994).
- [18] B.D. Day, Phys. Rev. Lett. **47**, 226 (1981).
- [19] A. Nogga, H. Kamada and W. Gloeckle, Phys. Rev. Lett. **85**, 944 (2000).
- [20] V. G. J. Stoks, R. A. M. Klomp, M. C. M. Rentmeester and J. J. de Swart, Phys. Rev. C **48**, 792 (1993).
- [21] M. Baldo, A. Fiasconaro, H. Q. Song, G. Giansiracusa and U. Lombardo, Phys. Rev. C **65**, 017303 (2002).
- [22] H. Q. Song, M. Baldo, G. Giansiracusa, and U. Lombardo, Phys. Rev. Lett. **81**, 1584 (1998).
- [23] H. Q. Song, M. Baldo, G. Giansiracusa, and U. Lombardo, Phys. Lett. **B473**, 1 (2000);
- [24] X. R. Zhou, G. F. Burgio, U. Lombardo, H.-J. Schulze, and W. Zuo, Phys. Rev. **C69**, 018801 (2004).
- [25] G.E. Brown, W. Weise, G. Baym and J. Speth, *Comm. Nucl. Part. Phys.* **17**, 39 (1987).
- [26] P. Bozek and P. Czerski, Acta Phys. Pol. B **34**, 2759 (2003).
- [27] Kh. Gad, Eur. Phys. J. A **22**, 405 (2004).